

# Fundamental limits on the rate of bacterial cell division

Nathan M. Belliveau<sup>†, 1</sup>, Griffin Chure<sup>†, 2, 3</sup>, Christina L. Hueschen<sup>4</sup>, Hernan G. Garcia<sup>5</sup>, Jane Kondev<sup>6</sup>, Daniel S. Fisher<sup>7</sup>, Julie A. Theriot<sup>1, 8</sup>, Rob Phillips<sup>2, 9, \*</sup>

\*For correspondence:

<sup>†</sup>These authors contributed equally to this work

<sup>1</sup>Department of Biology, University of Washington, Seattle, WA, USA; <sup>2</sup>Division of Biology and Biological Engineering, California Institute of Technology, Pasadena, CA, USA; <sup>3</sup>Department of Applied Physics, California Institute of Technology, Pasadena, CA, USA; <sup>4</sup>Department of Chemical Engineering, Stanford University, Stanford, CA, USA; <sup>5</sup>Department of Molecular Cell Biology and Department of Physics, University of California Berkeley, Berkeley, CA, USA; <sup>6</sup>Department of Physics, Brandeis University, Waltham, MA, USA; <sup>7</sup>Department of Applied Physics, Stanford University, Stanford, CA, USA; <sup>8</sup>Allen Institute for Cell Science, Seattle, WA, USA; <sup>9</sup>Department of Physics, California Institute of Technology, Pasadena, CA, USA; \*Contributed equally

**Abstract** This will be written next (promise).

## Relationship Between Cell Size and Growth Rate

The relationship between cell size and growth rate has long been of interest in the study of bacterial physiology, particularly following the now six decade-old observation that cell volume appears to increase exponentially with growth rate; known as Schaechter's growth law (Schaechter *et al.*, 1958; Taheri-Araghi *et al.*, 2015). However, the mechanism that governs this relationship, and even the question of whether the change in average cell size is truly exponential has remained under debate (Harris and Theriot, 2018). Given the importance of cell size in determining the total protein mass that must be doubled and in setting other parameters like the surface-area-to-volume ratio, we examine the proteomic data presented thus far data to consider cell size and growth rate.

At moderate growth rates (above about 0.5 hr<sup>-1</sup>), cells grow at a near-maximal rate near given their ribosomal mass fraction  $\Phi_R$  (??(B)). This means that in order to grow any faster, cells must increase  $\Phi_R$  further. A naïve strategy following the constraint of ?? is simply that cells should make additional ribosomes. In reality, however, large swaths of the proteome increase in absolute protein abundance as cells grow faster (Supplemental Figure X), and the ability to add additional ribosomes is likely constrained by other factors including crowding due to their large size (Delarue *et al.*, 2018; Soler-Bistué *et al.*, 2020). Instead, it is well-documented that *E. coli* cells add a constant volume per origin of replication, which is robust to a remarkable array of cellular perturbations (Si *et al.*, 2017). To consider this in the context of the proteomic data, we used the measurements from Si *et al.* (2017) for wild-type *E. coli* cells grown in different nutrient conditions (Figure 1(A)) to estimate the average number of origins per cell ( $\langle \# \text{ ori} \rangle$ ) across the data. Indeed, we find an approximately linear trend between protein copy number and  $\langle \# \text{ ori} \rangle$ , and in Figure 1(B) plot this for ribosomal copy numbers.

The average number of origins  $\langle \# \text{ ori} \rangle$  is set by how often replication must be initiated per cell doubling under steady-state growth, and can be quantified via

$$\langle \# \text{ ori} \rangle = 2^{\tau_{\text{cyc}}/\tau} = 2^{\tau_{\text{cyc}}\lambda/\ln(2)}, \quad (1)$$

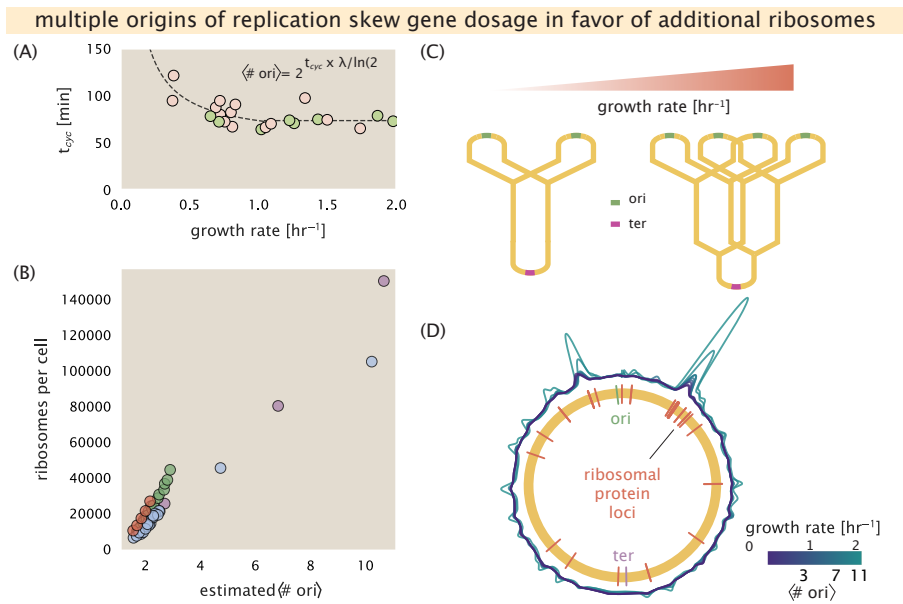


**Figure 1. Multiple replication initiations bias protein synthesis in favor of more ribosome.** (A) Experimental data from Si *et al.* (2017). Dashed line shows fit to the data, which were used to estimate  $\langle \# \text{ ori} \rangle$ .  $t_{cyc}$  was assumed to vary in proportion to  $\tau$  for doubling times great than 40 minutes, and then reach a minimum value of [fill in] minutes below this (see Supplemental Appendix X for additional details). Red data points correspond to measurements in strain MG1655, while light green points are for strain NCM3722. (B) Plot of the ribosome copy number estimated from the proteomic data against the estimated  $\langle \# \text{ ori} \rangle$ . (C) Schematic shows the expected increase in replication forks (or number of ori regions) as *E. coli* cells grow faster. (D) A running Gaussian average (20 kbp st. dev.) of protein copy number is calculated for each growth condition considered by (Schmidt *et al.*, 2016). Since total protein abundance increases with growth rate, protein copy numbers are median-subtracted to allow comparison between growth conditions.  $\langle \# \text{ ori} \rangle$  are estimated using the data in (A) and Equation 1. [still looking into how best to use this type of analysis]

where  $t_{cyc}$  is the cell cycle time (referring to the time from replication initiation to cell division), and  $\tau$  is the cell doubling time. For a constant cell cycle time, observed at growth rates above about 0.5 hr<sup>-1</sup> (Helmstetter and Cooper, 1968), Equation 1 says that  $\langle \# \text{ ori} \rangle$  will increase exponentially with the growth rate.

Insight into why cells add a constant volume per  $\langle \# \text{ ori} \rangle$ , and how this relates to growth, however, requires us to consider the changes in the proteome, and in particular ribosomal proteins across the different growth conditions. In Figure 1(D) we consider the position-dependent protein expression across the chromosome for each of the growth conditions from Schmidt *et al.* (2016). Here we calculated a running Gaussian average of protein copy number (20 kbp st. dev. averaging window) based on each gene's transcriptional start site, which were then median-subtracted to account for the differences in total protein abundance with each growth condition. Importantly, we find that the major deviations in protein copy number are largely restricted to regions of ribosomal protein genes, with substantially higher deviations observed for cells with high  $\langle \# \text{ ori} \rangle$  (teal), as compared to those with low  $\langle \# \text{ ori} \rangle$  (purple). This is particularly apparent for genes closer to the origin, where the majority of ribosomal proteins are found. This suggests that in addition to the linear scaling between protein abundance and  $\langle \# \text{ ori} \rangle$ , cells are also varying their relative ribosomal abundance in proportion to  $\langle \# \text{ ori} \rangle$ . Since growth rate depends specifically on the ribosomal fraction  $\Phi_R$ , this result suggests that cells are changing their size as a way to tune  $\Phi_R$  to match the available nutrient conditions.

While this dependence between cell size and ribosomal abundance is apparent across moderate to fast growth rates, it is worth noting that this scaling is likely to change at slow growth rates (below  $\lambda \approx 0.5$  hr<sup>-1</sup>). Here, the number of ribosomes  $R$  no longer reflects the cell's protein synthesis

capacity (*Dai et al., 2016*), so far taken to be  $r_i \times R$ , and instead, cells have an excess number of ribosomes. Additional regulatory control through the small-molecule alarmones such as guanosine pentaphosphate [(p)ppGpp] reduce the fraction of actively translating ribosomes at these slower growth rates. This overabundance of ribosomes provides different challenges on the ability of the cell to maintain steady-state growth under limiting nutrient conditions, and in Supplemental Section XX we consider this slow growth regime further.

As a final comment, it has recently been shown that growth in a (p)ppGpp null strain also lacked both the condition-dependent changes in  $\langle \# \text{ ori} \rangle$  as well as changes in cell size across different growth condition. Instead, cells always exhibited a high ratio of  $\langle \# \text{ ori} \rangle$  to  $\langle \# \text{ ter} \rangle$ , irrespective of growth rate, and a cell size that was more consistent with a fast growth state where (p)ppGpp levels are normally low (*Fernández-Coll et al., 2020*) and ribosomal fraction is high (*Zhu and Dai, 2019*). There is also evidence that this may be achieved through inhibition of DNA replication initiation (*Kraemer et al., 2019*). These observations raise the possibility that (p)ppGpp may be playing a causal role in tuning  $\langle \# \text{ ori} \rangle$  and cell size, which ultimately allows the cell to vary its ribosomal content according to nutrient availability.

[This last paragraph may be better placed in the discussion]

## [Header for final section??]

The relationship between cell size, actively translating ribosomes, and growth rate, suggest that cells tune their size and ribosomal abundance as a way to match their biosynthetic capacity to the available nutrient conditions. As one illustration of this, disruption of the major glucose uptake system PTS through the deletion of *ptsG* doesn't just simply limit carbon uptake and growth, which is reduced about two-fold. Rather, cells accommodate this perturbation by also reducing their ribosomal fraction about two-fold (*Dai et al., 2016*); matching the expected decrease in growth rate governed by ?? for this change in ribosomal fraction. In this final section we consider a minimal model of growth rate control. We use it to quantitatively show how changes in ribosomal content and total proteomic mass will allow cells to maximize their growth rate according to the available nutrient conditions.

To react to changes in nutrient conditions, bacteria rely on secondary-messenger molecules like (p)ppGpp, which cause global changes in transcriptional and translational activity. In *E. coli*, amino acid starvation causes the accumulation of deacylated tRNAs at the ribosome's A-site and this leads to a strong activation of (p)ppGpp synthesis activity by RelA (*Hauryliuk et al., 2015*). The dramatic decrease in active ribosomal fraction that is now apparent for growth rates below about  $0.5 \text{ hr}^{-1}$  ( $f_a \approx 0.5$  at a growth rate of about  $0.3 \text{ hr}^{-1}$ , *Dai et al. (2016)*) shows that (p)ppGpp also coordinates growth in poor nutrient conditions. Furthermore, (p)ppGpp can inhibit DNA replication initiation by mediating a change in transcriptional activity and the supercoiling state of the origin of replication (*Kraemer et al., 2019*). These observations all raise the possibility that it through (p)ppGpp that cells mediate the growth-rate dependent changes in  $\langle \# \text{ ori} \rangle$ , cell size and ribosomal abundance (*Zhu and Dai, 2019; Büke et al., 2020*). Indeed, recent work in a (p)ppGpp null strain found that cells exhibited a high ratio of  $\langle \# \text{ ori} \rangle$  to  $\langle \# \text{ ter} \rangle$  and cell size that was more consistent with a fast growth state where (p)ppGpp levels are normally low (*Fernández-Coll et al., 2020*).

To allow us to consider this hypothesis in light of our growth-rate dependent proteomic data, we proceed by assuming that the rate of elongation  $r_i$  depends only on the availability of amino acids (and, therefore, also amino-acyl tRNAs). It is through the synthesis and availability of amino acids that we will assume cells adjust their ribosomal abundance and cell size via (p)ppGpp. Other molecular players required for translation like elongation factors and GTP are considered in sufficient abundance, which appear to be valid assumptions given our analysis of the proteomic data and energy production thus far.

## A Minimal Model of Nutrient-Limited Growth

We begin by considering amino acids as a single species, with cellular concentration  $[AA]_{\text{eff}}$ . The rate of elongation  $r_t$  will depend on how quickly ribosomes can match codons with their correct amino-acyl tRNA, as well as the remaining steps required for peptide elongation. We therefore consider that elongation will depend on two course-grained timescales, 1) the time to find and bind each correct amino-acyl tRNA, and 2) the remaining steps in peptide elongation that will not depend on the amino acid availability. The time to translate each codon is given by the inverse of the elongation rate  $r_t$ , which can be written as,

$$\frac{1}{r_t} = \frac{1}{k_{\text{on}} B [AA]_{\text{eff}}} + \frac{1}{r_t^{\text{max}}}. \quad (2)$$

Here we have assumed that the rate of binding by amino-acyl tRNA  $k_{\text{on}}$  is proportional to  $[AA]_{\text{eff}}$  by a constant  $B$ . The second term on the right-hand side reflects our assumption that other steps in peptide elongation are not rate-limiting, with a maximum elongation rate  $r_t^{\text{max}}$  of about 17 aa per second *Dai et al. (2016)*. This can be rearranged more succinctly in terms of an effective binding constant  $K_d = r_t^{\text{max}} / (k_{\text{on}} B)$ , with the elongation rate now given by,

$$r_t = \frac{r_t^{\text{max}}}{1 + K_d / [AA]_{\text{eff}}}. \quad (3)$$

During steady-state growth the amino acid concentration is constant ( $d[AA]_{\text{eff}}/dt=0$ ).  $[AA]_{\text{eff}}$  will relate to the rate of amino acid synthesis (or import, for rich media)  $r_{aa}$  and consumption  $r_t R f_a$  by,

$$\int_0^\tau \frac{d[AA]_{\text{eff}}}{dt} dt = \int_0^\tau ([r_{aa}] - [r_t R f_a]) dt, \quad (4)$$

where the time from 0 to  $\tau$  is a single cell doubling, and the square brackets indicate of concentration per time. Solving this, we find that

$$[AA]_{\text{eff}} = ([r_{aa}] - [r_t R f_a]) \tau. \quad (5)$$

Alternatively, for an average cell size of  $V$ ,  $[r_{aa}] = r_{aa} / (V N_A)$  and  $[r_t R f_a] = (r_t R f_a) / (V N_A)$ , where  $N_A$  is Avogadro's number. Since  $\tau = \ln(2) / \lambda$ , which is also related to the parameters  $r_t R f_a$  and  $N_{aa}$  through ??, we can also rewrite this as,

$$[AA]_{\text{eff}} = \frac{\ln(2) N_{aa}}{V N_A} \left( \frac{r_{aa}}{r_t R f_a} - 1 \right). \quad (6)$$

By plugging in **Equation 6** into **Equation 3**, which also depends on  $r_t$ , we can solve for  $r_t$  explicitly. Its solution are the roots of a quadratic equation, with the positive given by,

$$r_t = \frac{\sqrt{c^2 + 4ckr_t^{\text{max}} - 2cr_t^{\text{max}} + (r_t^{\text{max}})^2} - c - r_t^{\text{max}}}{2(k-1)}. \quad (7)$$

Here,  $c = r_{aa} / (R f_a)$  and  $k = N_A V K_d / N_{aa}$ . In the final two subsections we use this model to explore how the cell's metabolic capacity ( $r_{aa}$ ) constrains the maximum growth rate, and then explain an apparent role of for (p)ppGpp in mitigating translational activity at slow growth, where the number of ribosomes is in excess.

## Optimal Growth Rate, Ribosomal Content, and Cell Size Depend on Nutrient Availability and Metabolic Capacity.

The way we will explore this model is to constrain the set of parameters based on those observed for *E. coli* under nutrient limitation; namely, we will restrict the values of  $R$ ,  $N_{aa}$ , and  $V$  to those associated with the growth conditions in *Schmidt et al. (2016)*. We will then consider how changes in the nutrient conditions, through the parameter  $r_{aa}$ , influence the maximum growth rate. In **Figure 2(A)** we begin by plotting the elongation rate  $r_t$  for a high and low value of  $r_{aa}$ , reflective of poor and rich nutrient conditions, respectively as a function of cellular ribosome concentration

**Figure 2.** (A) (B)

---

144 [NB: need to state values used - maybe rationalize choice of values based on the data]. Here we  
145 find that for high values of  $r_{aa}$ , cells will be able to support protein synthesis and maintain a high  
146 rate of elongation. However, for poor nutrient conditions (low  $r_{aa}$ ), a high abundance of ribosomes  
147 causes a dramatic decrease in  $r_i$ . In this regime, we see that a reduction of actively translating  
148 ribosomes, through the parameter  $f_a$ , allow cells to maintain a high rate of elongation even ...

## References

- Büke, F., Grilli, J., Lagomarsino, M. C., Bokinsky, G., and Tans, S. (2020). ppGpp is a bacterial cell size regulator. *bioRxiv*, 266:2020.06.16.154187.
- Dai, X., Zhu, M., Warren, M., Balakrishnan, R., Patsalo, V., Okano, H., Williamson, J. R., Fredrick, K., Wang, Y.-P., and Hwa, T. (2016). Reduction of translating ribosomes enables *Escherichia coli* to maintain elongation rates during slow growth. *Nature Microbiology*, 2(2):16231.
- Delarue, M., Brittingham, G. P., Pfeffer, S., Surovtsev, I. V., Pinglay, S., Kennedy, K. J., Schaffer, M., Gutierrez, J. I., Sang, D., Poterewicz, G., Chung, J. K., Plitzko, J. M., Groves, J. T., Jacobs-Wagner, C., Engel, B. D., and Holt, L. J. (2018). mTORC1 Controls Phase Separation and the Biophysical Properties of the Cytoplasm by Tuning Crowding. *Cell*, 174(2):338–349.e20.
- Fernández-Coll, L., Maciag-Dorszynska, M., Tailor, K., Vadia, S., Levin, P. A., Szalewska-Palasz, A., Cashel, M., and Dunny, G. M. (2020). The Absence of (p)ppGpp Renders Initiation of *Escherichia coli* Chromosomal DNA Synthesis Independent of Growth Rates. *mBio*, 11(2):45.
- Harris, L. K. and Theriot, J. A. (2018). Surface Area to Volume Ratio: A Natural Variable for Bacterial Morphogenesis. *Trends in microbiology*, 26(10):815–832.
- Hauryluk, V., Atkinson, G. C., Murakami, K. S., Tenson, T., and Gerdes, K. (2015). Recent functional insights into the role of (p)ppGpp in bacterial physiology. *Nature Reviews Microbiology*, 13(5):298–309.
- Helmstetter, C. E. and Cooper, S. (1968). DNA synthesis during the division cycle of rapidly growing *Escherichia coli* Br. *Journal of Molecular Biology*, 31(3):507–518.
- Kraemer, J. A., Sanderlin, A. G., and Laub, M. T. (2019). The Stringent Response Inhibits DNA Replication Initiation in *E. coli* by Modulating Supercoiling of oriC. *mBio*, 10(4):822.
- Schaechter, M., Maaløe, O., and Kjeldgaard, N. O. (1958). Dependency on Medium and Temperature of Cell Size and Chemical Composition during Balanced Growth of *Salmonella typhimurium*. *Microbiology*, 19(3):592–606.
- Schmidt, A., Kochanowski, K., Vedelaar, S., Ahrné, E., Volkmer, B., Callipo, L., Knoops, K., Bauer, M., Aebersold, R., and Heinemann, M. (2016). The quantitative and condition-dependent *Escherichia coli* proteome. *Nature Biotechnology*, 34(1):104–110.
- Si, F., Li, D., Cox, S. E., Sauls, J. T., Azizi, O., Sou, C., Schwartz, A. B., Erickstad, M. J., Jun, Y., Li, X., and Jun, S. (2017). Invariance of Initiation Mass and Predictability of Cell Size in *Escherichia coli*. *Current Biology*, 27(9):1278–1287.
- Soler-Bistué, A., Aguilar-Pierlé, S., Garcia-Garcera, M., Val, M.-E., Sismeiro, O., Varet, H., Sieira, R., Krin, E., Skovgaard, O., Comerchi, D. J., Eduardo P. C. Rocha, and Mazel, D. (2020). Macromolecular crowding links ribosomal protein gene dosage to growth rate in *Vibrio cholerae*. *BMC Biology*, 18(1):1–18.
- Taheri-Araghi, S., Bradde, S., Sauls, J. T., Hill, N. S., Levin, P. A., Paulsson, J., Vergassola, M., and Jun, S. (2015). Cell-size control and homeostasis in bacteria. - PubMed - NCBI. *Current Biology*, 25(3):385–391.
- Zhu, M. and Dai, X. (2019). Growth suppression by altered (p)ppGpp levels results from non-optimal resource allocation in *Escherichia coli*. *Nucleic Acids Research*, 47(9):4684–4693.